

The third UltraVISTA data release

N. Boufflos, O. Herent, P. Hudelot, H. J. McCracken, Y. Mellier
(TERAPIX/Institut d’Astrophysique de Paris);
J. Dunlop, O. Le Fèvre, M. Franx, J. Fynbo,
R. Bowler, K. Caputi, A. Muzzin, B. Milvang-Jensen, J. Zabl (UltraVISTA);
E. Gonzalez-Solares, M. Irwin, J. Lewis (CASU).

March 17, 2016

Data Collection: UltraVISTA
Release number 3
Data provider: Jim Dunlop
Date: March 17, 2016

1 Abstract

UltraVISTA is an ultra-deep near-infrared survey of the central region of the COSMOS field (Scoville et al. 2007). This document describes the third UltraVISTA data release, “DR3” which comprises stacked images and catalogues in $YJHK_s$ and the NB118 narrow-band filter. The principal difference with respect to the DR1 and DR2 releases is a substantial increase in exposure time in the four “ultra-deep stripes” regions (see Table 1).

1.1 Acknowledging these data products

Any publications using these data products must include this text.

“Based on data products from observations made with ESO Telescopes at the La Silla Paranal Observatory under ESO programme ID 179.A-2005 and on data products produced by TERAPIX and the Cambridge Astronomy Survey Unit on behalf of the UltraVISTA consortium.”

In addition a reference to the UltraVISTA DR1 survey paper should be included: McCracken et al. (2012).

2 Overview of observations

DR3 contains all pre-processed UltraVISTA images from CASU (“The Cambridge Astronomy Survey Unit”¹) from 4th December, 2009 to 31st May 2014 as available in August 2014. The observation dates of all the 40,250 individual images used can be found by inspecting the file names of the individual images which are recorded in the provenance tables stored in an extension

¹<http://casu.ast.cam.ac.uk>

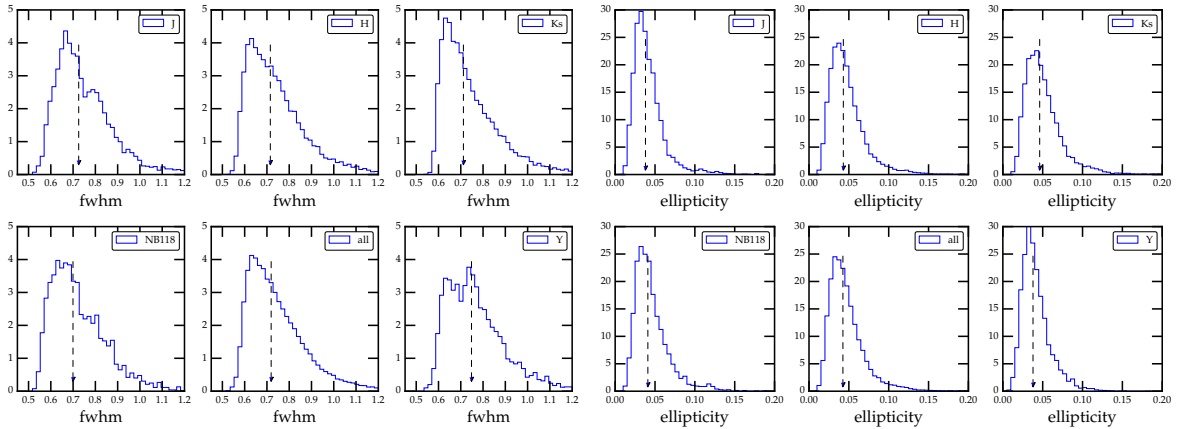


Figure 1: Seeing (left) and ellipticity (right) distributions for all UltraVISTA images in DR3. The arrow represents the median of each distribution.

in each image, described in Section 5.1. The total number of observing blocks contributing to this release is 1157. The total exposure time in this release is 898 hours.

This release comprises five complete observing seasons: however, very little data was taken in 2010 – 2011 due to the VISTA primary mirror being re-coated during the UltraVISTA observing season. Figure 1 shows the seeing and ellipticity distributions (measured using the PSFex) of all images which were processed for DR3, separated by filter. The dotted line represents the median of each distribution. In general, the median values in each filter are very similar, a consequence of the queue scheduled observations.

3 Release Content

3.1 Overview

In this release we provide five stacked images and their corresponding weight maps for Y , J , H , K_s , and NB118 narrow-band data taken during first five years of UltraVISTA survey operations. In addition, single band individual source lists and source lists created in dual-image mode (using the K_s image as a detection image) are provided (note that in ESO terminology, single-band tabular data are referred to as “Source lists” and multi-band merged data are referred to as catalogues). We also provide a five-band catalogue that meets the requirement for a “catalogue” in the Phase 3 framework. Total data volume is unchanged from previous release, i.e., ~ 90 Gb in total, including catalogues. The total survey area is 1.8 deg^2 and 1.7 deg^2 after masking.

3.2 Special image header contents

Some new metadata has been added to the image headers following the Phase 3 standard. For example, EXPTIME and ABMAGLIM header keywords contain the value for the ultra-deep stripes, whereas the values for the deep stripes are given in the comment header lines. This is the same

scheme used in DR2. Here is an example of the relevant lines of the K_s header:

```
EXPTIME = 504820.1 / Total integration time per pixel (s)
...
ABMAGLIM= 24.9 / 5-sigma limiting AB magnitude for point sources
...
COMMENT ultra-deep stripes: typ. exptime per px = 504820.1 s (keyword EXPTIME)
COMMENT deep stripes: typ. exptime per px = 41200.0 s
COMMENT ultra-deep stripes: typical ABMAGLIM = 24.9 (keyword ABMAGLIM)
COMMENT deep stripes: typical ABMAGLIM = 23.8
```

We have also added DIT and NDIT keywords only to the stacks where all the individual images had the same value of DIT and or NDIT. For all stacks we give in COMMENT header fields information about the breakdown of the individual images on DIT and NDIT, for example for the H -band stack:

```
COMMENT Breakdown of the used images on different NDIT,DIT combinations
COMMENT N_images NDIT DIT
COMMENT      2349   10   6
COMMENT      10928   6  10
```

All of the observing blocks which contributed to each stacked image are listed in the OBID parameter in the header.

4 Release notes

4.1 Data reduction and calibration

In August 2014 we downloaded from CASU² all available individual sky-subtracted images, the corresponding sky frames, flat-fields, bad pixel maps and stacked `_st` images. At this initial stage, no selection was applied. We created our own weight-maps from the supplied flat-fields and bad pixel maps. Note that this image selection also includes data we had already processed for the DR1 and DR2 releases; however these images had since been re-processed by a new version of the CASU pipeline (version 1.3) and we wished also to take advantage of improvements in the TERAPIX pipeline.

All DR1 images had been visually inspected. During this inspection process we found that a small number of images taken early in the survey had doubled point-spread-functions due to the loss of auto-guiding; these problems were since resolved and do not affect subsequent data. We preserved the grades from the DR1 processing and used it to reject the images with failed auto-guiding present in DR3.

Image processing techniques followed methods outlined in DR1 (McCracken et al. 2012) and in the DR2 survey release document. To briefly summarise: we first generate source lists and weight maps from the initial CASU sky-subtracted data and generate first-pass stacks. These first-pass stacks are used to generate object masks which are then used to compute sky frames

²<http://casu.ast.cam.ac.uk/vistasp/>

for each of the individual images. The sky frames are subtracted from the individual images (after the sky-frames generated by CASU are first added back). De-stripping (in both x - and y - directions) is carried out as well as a large-scale gradient removal before weight-maps and source lists are re-generated once more for each individual images. Once astrometric solutions are computed, the images are coadded to the final COSMOS astrometric grid using a pre-defined tangent point. We use the same techniques as in DR2 to co-add the images: a full description can be found in the DR2 release document³. One notable change is that for this release we generate sigma-clipped stacks using the “official” version 2.36.1 of `Swarp`⁴, which now includes a sigma-clipping combination option. This gives results identical to the (unsupported) version of `Swarp` used previously.

4.2 Change of astrometric reference catalogue and a new method to compute the astrometric solution

Since the start of the involvement of TERAPIX in the COSMOS project, we have used an astrometric catalogue derived from Megacam i^* band images taken over the full COSMOS field. These images were in turn registered to an external astrometric reference frame. Since then, 2MASS (Skrutskie et al. 2006) has become available and the limitations of the earlier catalogue have become apparent (for example, there is an offset in declination visible in the lower panel in Figure 7 of McCracken et al. (2012)). For DR3 we have switched to a new astrometric catalogue based on Pan-STARRS Medium-Deep Survey data kindly provided to us by G. Hasinger. To create this catalogue, we coadded Pan-Starrs tiles to make a single large image covering COSMOS and then extracted a reference catalogue for use with `Scamp` using `SExtractor`. These images and catalogues are being made public for other spectroscopic surveys which require dense astrometric catalogues in the COSMOS field.

One challenge of using `Scamp` to compute astrometric solutions for UltraVISTA is that the number of images varies significantly over the field. The “deep stripe” areas have a much larger integration time per pixel than the wide area. Consequently, the relative astrometric weight between the internal and external catalogues varies across the field-of-view (with deep stripe regions containing many more overlapping exposures). This in turn creates oscillations and discontinuities in the astrometric solution compared to the external astrometric solutions. In order to solve this problem we changed how we computed our astrometric solution with `Scamp` by using a specific “context” corresponding to the “paw” (observing location) used. Of course, a simpler, but non-optimal solution, would be simply to ignore the overlapping images and tie all frames to the external reference. However, this approach discards information provided by the overlapping images. By adopting a separate context for each observing position, the different amount of images at each overlapping position are handled correctly.

The combination of these two changes means that in DR3 our astrometric solutions, both internally and externally, are much better than one pixel (0.1”) over the full UltraVISTA field in all five bands, and are free from any kind of systematic effects internally. This represents a significant improvement over previous releases, and ensures that we will be able to maintain this high astrometric quality in the future.

³http://www.eso.org/sci/observing/phase3/data_releases/uvista_dr2.pdf

⁴<http://www.astromatic.net/software/swarp>

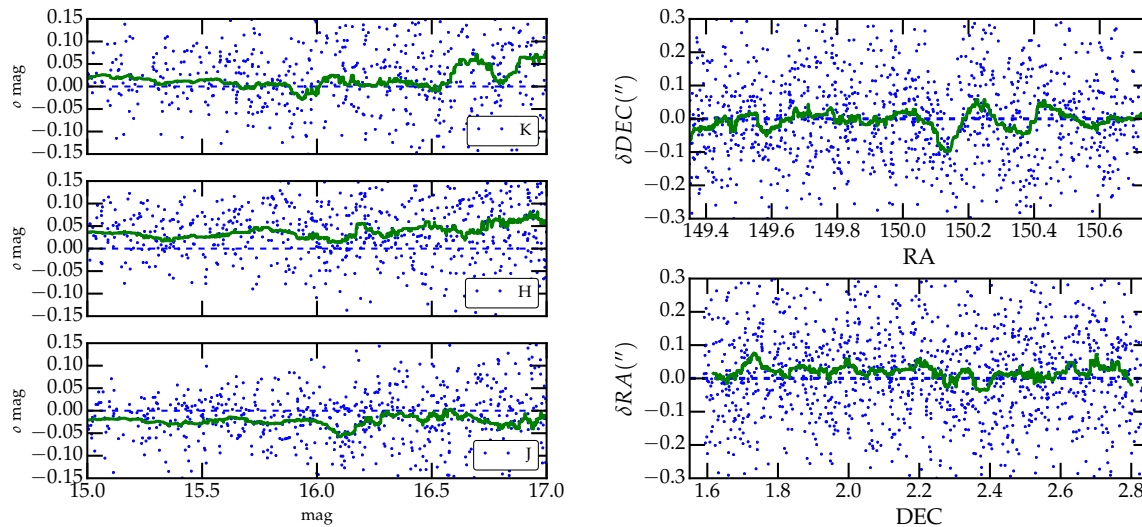


Figure 2: Comparisons with 2MASS. Left panel: Magnitude difference δ between total J , H , and K_s magnitudes of stars in UltraVISTA DR3 with sources in 2MASS. The green line corresponds to a running median computed over 100 points. Right panel: Difference in position, in arcseconds, with respect to stars in the 2MASS, as a function of right ascension and declination (upper and lower panels respectively); every second point is plotted. The solid line shows a running median.

4.3 Data quality

4.3.1 Comparison with 2MASS

In Figure 2 we compare the `mag_auto` magnitudes and positions of stars in our source list with those in the 2MASS all-sky point source catalogue (Skrutskie et al. 2006). (Note also that 2MASS is used for the initial photometric calibration of the survey by CASU.) Of course, a significant limitation of this comparison is that the magnitude range over which sources in UltraVISTA and 2MASS overlap is relatively small, and furthermore that the UltraVISTA instrumental photometric system is not the same as the 2MASS system (this is described in more detail in McCracken et al.).

Nevertheless, the result of this test is shown in the left panel of Fig. 2 where we plot UltraVISTA-2MASS magnitudes for all non-saturated stellar sources and for a total photometric error in (2MASS and UltraVISTA, summed in quadrature) of less than 0.2mag. The thick solid line shows a running median which is always within approximately 0.05 magnitudes of zero for $15.0 < \text{mag} < 17.0$. These curves are very similar to those plotted in McCracken et al., considering the uncertainties in the 2MASS photometry at these magnitudes.

In the right panel of Fig. 2 we compare the positions in right ascension and declination of point sources in 2MASS with those in our UltraVISTA K_s catalogue. Since we have changed our astrometric reference catalogue compared to DR1 and DR2, the small offset in DEC compared to 2MASS has now been removed.

| Filter | Exposure time (hrs) | | Limiting mag. $5\sigma(2'')$ | |
|----------------------|------------------------|------|---------------------------------|------|
| | Ultra-deep | Deep | Ultra-deep | Deep |
| <i>Y</i> | 106.5 | 11.1 | 25.7 | 24.8 |
| <i>J</i> | 102.6 | 12.4 | 25.4 | 24.5 |
| <i>H</i> | 134.2 | 13.4 | 25.1 | 24.1 |
| <i>K_s</i> | 140.2 | 11.4 | 24.9 | 23.8 |
| NB118 | 66.8 | - | 24.1 | - |

Table 1: Characteristics of the images: typical exposure time per pixel and limiting magnitudes in both deep and ultra-deep regions. **Important note:** The limiting magnitudes listed in this table and in the headers are computed using “empty aperture” measurements in $2.0''$ diameter apertures, and are subsequently corrected to total magnitude by subtracting 0.3 mag. This 0.3 mag aperture correction was also used in the DR2 headers, but not in the table in the DR2 release document.

4.3.2 Limiting magnitudes and seeing

Limiting magnitudes are computed identically as in McCracken et al.: first, `SEXtractor` is run on each stack using the same detection threshold parameters as used for catalogue generation. All pixels belonging to objects to this detection limit are flagged. Next, we measure fluxes in apertures of diameter $2''$ over the entire mosaic; any aperture which contains object pixels is discarded. The limiting magnitude is then simply computed from the standard deviation of fluxes measured in these apertures. These measurements were carried out on each stripe in all bands for all images. Our measurements are summarised in Table 1.

We measured the seeing on all the stacks using `PSFex`. The seeing in the *YJHK_s* NB118 bands is $(0.8, 0.8, 0.7, 0.7, 0.7)''$ respectively, with a mean stellar ellipticity on all bands of ~ 0.01 .

4.4 Known issues

As a consequence of the varying exposure time between the different stripes, it is impossible to assign a single gain value appropriate for the entire image. For this reason, no `GAIN` keyword is included in the image headers. Furthermore, because of the change in astrometric reference frame, COSMOS data products in other bands may need to be resampled to properly align with this data. As explained in Section 4.2 this release uses a new astrometric reference catalogue, and there may a small offset with respect to the previous COSMOS data products. We expect to eventually resample all COSMOS data products onto this new reference frame.

4.5 Previous releases

This release supersedes DR1 and DR2. The depth in this release has substantially increased in the ultra-deep stripes.

| Software name | Version |
|----------------------------|---------|
| <code>SExtractor</code> | 2.18.12 |
| <code>SWarp</code> | 2.36.1 |
| <code>PSFex</code> | 3.15.2 |
| <code>WeightWatcher</code> | 1.10 |
| <code>MissFITS</code> | 2.60 |
| <code>SCamp</code> | 2.0b11 |

Table 2: Software versions used in UltraVISTA DR3.

4.6 Software versions

DR3 makes extensive use of the `astromatic` set of software tools. A complete list of software versions which were used in this release is given in Table 2.

5 Data format

5.1 File types

All images and catalogues are distributed in FITS format. In this release, we provide five stacked images and their corresponding weight maps for Y , J , H , K_s , and NB118 narrow-band data composed of images from the first five years of the UltraVISTA public survey.

Given the deep and ultra-deep sections have considerably different exposure times, this has the important consequence that the signal-to-noise ratio for an object of a given magnitude will vary across the image. An inspection of the weight map provided with each image will indicate the location of the deeper zones.

Images have a zero-point of 30.0 AB magnitudes for a one second equivalent exposure time. The conversion AB-Vega follows the offsets given in McCracken et al. (2015). The images have a pixel scale of $0.15''/\text{pixel}$ and have a common tangent point, in decimal RA, DEC (J2000) of (150.116,2.2000). This is the tangent point of the publicly available IRSA/COSMOS images. Each image is $\sim 9\text{Gb}$ in size.

Following the ESO Phase 3 standard, the FITS files for the 5 stacks are multi-extension FITS files, with the stacked image in the primary HDU (header data unit) and with a “provenance table” in the first (and only) extension. The provenance table lists all the raw images that — after processing at CASU and TERAPIX — were combined to make the given stack. The FITS files for the weight maps for the stacks have the same provenance tables as the FITS files for the stacks.

5.2 Complete list of distributed products

Tables 3 and 4 lists the imaging and source list data products distributed in DR3. Five images are provided, as well as their corresponding weight maps. These weight-maps correspond to

| Filename | Description |
|---|--------------------|
| UVISTA_Y_21_01_16_allpaw_skysub_015_dr3_rc_v5.fits | Y-band stack |
| UVISTA_Y_21_01_16_allpaw_skysub_015_dr3_rc_v5.weight.fits | Y-band weight |
| UVISTA_J_21_01_16_allpaw_skysub_015_dr3_rc_v5.fits | J-band stack |
| UVISTA_J_21_01_16_allpaw_skysub_015_dr3_rc_v5.weight.fits | J-band weight |
| UVISTA_H_21_01_16_allpaw_skysub_015_dr3_rc_v5.fits | H-band stack |
| UVISTA_H_21_01_16_allpaw_skysub_015_dr3_rc_v5.weight.fits | H-band weight |
| UVISTA_Ks_21_01_16_allpaw_skysub_015_dr3_rc_v5.fits | K_s -band stack |
| UVISTA_Ks_21_01_16_allpaw_skysub_015_dr3_rc_v5.weight.fits | K_s -band weight |
| UVISTA_NB118_21_01_16_allpaw_skysub_015_dr3_rc_v5.fits | NB118-band stack |
| UVISTA_NB118_21_01_16_allpaw_skysub_015_dr3_rc_v5.weight.fits | NB118-band weight |

Table 3: Summary of DR3 stacked images. All images have a zero point of 30.0 AB magnitudes for a one second equivalent exposure time and a scale of $0.15''/\text{pixel}$.

the `MAP_WEIGHT` images produced by `swarp` and have pixel values proportional to the inverse variance.

We provide several source list products: “dual-mode” ones, in which the K_s image is used as the detection image and each of the other images in turn is used as the measurement image; and “single band” images in which each individual image is used in turn as both measurement and detection image. Dual-mode source lists have the advantage that, as the same number of entries is present in all catalogues, colours can be easily computed for each object. The second catalogue type contains, in principle, all sources to a given detection threshold (1.8σ). Catalogues were extracted using `SExtractor` (Bertin & Arnouts 1996) version 2.19.5 compiled and downloaded from the public SVN on astromatic.net⁵ (note that this is different than the version of `SExtractor` used during the pipeline processing which is listed in Table 2). For each entry in the source list we provide flux measurements in 18 photometric apertures. Their diameters in pixels are as follows, corresponding to three apertures of $2''$, $3''$ and $7.1''$ and logarithmically spaced apertures from $0.5''$ to $5''$:

13.33, 20.00, 47.33, 3.33, 3.93, 4.63, 5.46, 6.44, 7.59, 8.94, 10.54,
12.43, 14.65, 17.26, 20.35, 23.99, 28.28, 33.33.

We also provide a merged 5-band catalogue `UVISTA_5band_cat_dr3_rc_v5.fits` created from these individual K_s -selected catalogues. The columns in this catalogue are described in Table 5. Two additional columns are provided: the $E(B - V)$ Galactic reddening value measured at the position of each galaxy in the Schlegel et al. (1998) dust maps, together with a flag which indicates the field border.

⁵<http://www.astromatic.net/repositories>

| Filename | Detection | Measurement |
|---|-----------|----------------|
| UVISTA_Ks_21_01_16_allpaw_skysub_015_dr3_rc_v5.cat.fits | K_s | K_s |
| UVISTA_Ks_21_01_16_allpaw_skysub_015_dr3_rc_v5_Y.cat.fits | K_s | Y |
| UVISTA_Ks_21_01_16_allpaw_skysub_015_dr3_rc_v5_J.cat.fits | K_s | J |
| UVISTA_Ks_21_01_16_allpaw_skysub_015_dr3_rc_v5_H.cat.fits | K_s | H |
| UVISTA_Ks_21_01_16_allpaw_skysub_015_dr3_rc_v5_NB118.cat.fits | K_s | NB118 |
| UVISTA_Y_21_01_16_allpaw_skysub_015_dr3_rc_v5.cat.fits | Y | Y |
| UVISTA_J_21_01_16_allpaw_skysub_015_dr3_rc_v5.cat.fits | J | J |
| UVISTA_H_21_01_16_allpaw_skysub_015_dr3_rc_v5.cat.fits | H | H |
| UVISTA_NB118_21_01_16_allpaw_skysub_015_dr3_rc_v5.cat.fits | NB118 | NB118 |
| UVISTA_5band_cat_dr3_rc_v5.fits | K_s | $YJHK_s$ NB118 |

Table 4: Source list and catalogue products delivered with DR3.

6 Acknowledgements

H. J. McCracken acknowledges the use of TERAPIX computing facilities and support of the PNCG. This research has made use of the Vizier catalogue access tool provided by the CDS, Strasbourg, France. JPUF and BMJ acknowledge support from the ERC-StG grant EGG-278202. The Dark Cosmology Centre is funded by the Danish National Research Foundation. OLF, CSJ, LT acknowledge support from the ERC advanced grant ERC-2010-AdG-268107. JH acknowledges support from NWO. JSD acknowledges the support of the Royal Society via a Wolfson Research Merit award, and also the support of the European Research Council via the award of an Advanced Grant. The UltraVISTA team would like to thank ESO staff for scheduling and making the UltraVISTA observations, and the Cambridge Astronomy Survey Unit for providing us with pre-processed UltraVISTA images. We thank G. Hasinger for supplying us with the Pan-STARRS images used here, and E. Bertin for many useful discussions concerning the usage of the `Astromatic` tool set.

References

- Bertin, E. & Arnouts, S. 1996, *ApJS*, 117, 393
- McCracken, H. J., Milvang-Jensen, B., Dunlop, J., et al. 2012, *A&A*, 544, A156
- McCracken, H. J., Wolk, M., Colombi, S., et al. 2015, *MNRAS*, 449, 901
- Schlegel, D. J., Finkbeiner, D. P., & Davis, M. 1998, *ApJ*, 500, 525
- Scoville, N., Aussel, H., Brusa, M., et al. 2007, *ApJS*, 172, 1
- Skrutskie, M. F., Cutri, R. M., Stiening, R., et al. 2006, *AJ*, 131, 1163

| Column number | Column name | Description |
|---------------|--------------------|--|
| 1 | SOURCE_ID* | UltraVISTA source designation (DR3) |
| 2 | NUMBER* | Running object number |
| 3 | ALPHA_J2000* | Right ascension of barycenter in decimal degrees (J2000) |
| 4 | DELTA_J2000* | Declination of barycenter in decimal degrees (J2000) |
| 5 | X_IMAGE* | Object position along x |
| 6 | Y_IMAGE* | Object position along y |
| 7 | FLAG_HJMCC* | Bad region flag: != 0 for bad region (field boundaries: 1) |
| 8 | EBV* | Galactic reddening E(B-V) based on Schlegel et al (1998) dust maps |
| 9 | Y_APER2* | Y fixed aperture magnitude (2") |
| 10 | Y_APER2_ERR* | Y fixed aperture mag error (2") |
| 11 | Y_APER7* | Y fixed aperture magnitude (7.1") |
| 12 | Y_APER7_ERR* | Y fixed aperture mag error (7.1") |
| 13 | Y_AUTO* | Y auto magnitude |
| 14 | Y_AUTO_ERR* | Y auto mag error |
| 15 | Y_FLUX_RADIUS* | Radius of aperture containing half the flux of Y_MAG_AUTO |
| 16 | Y_FLAG* | Y Flag (sextractor) |
| 17 | J_APER2* | J fixed aperture magnitude (2") |
| 18 | J_APER2_ERR* | J fixed aperture mag error (2") |
| 19 | J_APER7* | J fixed aperture magnitude (7.1") |
| 20 | J_APER7_ERR* | J fixed aperture mag error (7.1") |
| 21 | J_AUTO* | J auto magnitude |
| 22 | J_AUTO_ERR* | J auto mag error |
| 23 | J_FLUX_RADIUS* | Radius of aperture containing half the flux of J_MAG_AUTO |
| 24 | J_FLAG* | J Flag (sextractor) |
| 25 | H_APER2* | H fixed aperture magnitude (2") |
| 26 | H_APER2_ERR* | H fixed aperture mag error (2") |
| 27 | H_APER7* | H fixed aperture magnitude (7.1") |
| 28 | H_APER7_ERR* | H fixed aperture mag error (7.1") |
| 29 | H_AUTO* | H auto magnitude |
| 30 | H_AUTO_ERR* | H auto mag error |
| 31 | H_FLUX_RADIUS* | Radius of aperture containing half the flux of H_MAG_AUTO |
| 32 | H_FLAG* | H Flag (sextractor) |
| 33 | KS_APER2* | Ks fixed aperture magnitude (2") [detection image] |
| 34 | KS_APER2_ERR* | Ks fixed aperture mag error (2") [detection image] |
| 35 | KS_APER7* | Ks fixed aperture magnitude (7.1") [detection image] |
| 36 | KS_APER7_ERR* | Ks fixed aperture mag error (7.1") [detection image] |
| 37 | KS_AUTO* | Ks auto magnitude [detection image] |
| 38 | KS_AUTO_ERR* | Ks auto mag error [detection image] |
| 39 | KS_FLUX_RADIUS* | Radius of aperture containing half the flux of KS_MAG_AUTO |
| 40 | KS_FLAG* | Ks Flag (sextractor) [detection image] |
| 41 | NB118_APER2* | NB118 fixed aperture magnitude |
| 42 | NB118_APER2_ERR* | NB118 fixed aperture mag error |
| 43 | NB118_APER7* | NB118 fixed aperture magnitude |
| 44 | NB118_APER7_ERR* | NB118 fixed aperture mag error |
| 45 | NB118_AUTO* | NB118 auto magnitude |
| 46 | NB118_AUTO_ERR* | NB118 auto mag error |
| 47 | NB118_FLUX_RADIUS* | Radius of aperture containing half the flux of NB118_MAG_AUTO |
| 48 | NB118_FLAG* | NB118 Flag (sextractor) |

Table 5: Complete list of parameters in the five-band merged catalogue. All magnitudes are in the AB system.